Aggregation properties of nitroporphyrins: Comparisons between solid-state and solution structures

ARTICLE *in* INORGANIC CHEMISTRY · JUNE 1993

Impact Factor: 4.76 · DOI: 10.1021/ic00066a027

6 AUTHORS, INCLUDING:

Mathias O. Senge
Trinity College Dublin
375 PUBLICATIONS **5,828** CITATIONS

SEE PROFILE

W. Robert Scheidt
University of Notre Dame
363 PUBLICATIONS **13,272** CITATIONS

SEE PROFILE

Aggregation Properties of Nitroporphyrins: Comparisons between Solid-State and Solution Structures

Mathias O. Senge,[1a] Charles W. Eigenbrot,[1b] Theodore D. Brennan,[1b] Janine Shusta,[1b] W. Robert Scheidt,*[1b] and Kevin M. Smith*[1a]

Departments of Chemistry, University of California, Davis, California 95616, and University of Notre Dame, Notre Dame, Indiana 46556

Received December 8, 1992

Previous NMR spectroscopic studies on the aggregation properties of metalloporphyrins suggested that monosubstituted octaethylporphyrin (OEP) derivatives with substituents capable of inducing charge polarization form tail-to-tail type dimers in solution. Such dimers have implications as model compounds for the photosynthetic reaction center. Crystallographic studies on a series of 5-NO_2-OEP compounds show that the zinc(II) complexes can indeed form dimers of the proposed type in the solid state. A four-coordinated planar zinc(II) 5-nitrooctaethylporphyrin and the corresponding methanol complex showed strong aggregation in the solid state. The pyridine complex and the free-base porphyrin showed no strong aggregation. Crystal data: 5-NO_2-OEP (**7**), $C_{36}H_{45}N_5O_2$, M_r = 579.8, triclinic, $P\bar{1}$, a = 9.374(3) Å, b = 13.794(6) Å, c = 14.221(4) Å, α = 104.69(3)°, β = 106.39(2)°, γ = 104.57(3)°, V = 1599.7(10) Å^3, Z = 2, D_x = 1.204 Mg·m^{-3}, λ(Mo Kα) = 0.710 73 Å, μ = 0.080 mm^{-1}, 130 K, R = 0.078 for 3328 reflections with $F > 3.5\sigma(F)$; Zn(5-NO_2-OEP)(C_5H_5N) (**9**-C_5H_5N), $C_{41}H_{48}N_6O_2Zn$, M_r = 722.6, triclinic, $P\bar{1}$, a = 9.942(3) Å, b = 10.722(4) Å, c = 17.744(5) Å, α = 81.74(3)°, β = 78.67(3)°, γ = 83.99(3)°, V = 1829.5(8) Å^3, Z = 2, D_x = 1.32 Mg·m^{-3}, λ(Mo Kα) = 0.710 73 Å, μ = 0.731 mm^{-1}, 293 K, R = 0.063 for 5161 reflections with $F > 3\sigma(F)$; Zn(5-NO_2-OEP) (**9**), $C_{36}H_{43}N_5O_2Zn$, M_r = 643.15, monoclinic, $P2_1/c$, a = 9.721(3) Å, b = 21.807(6) Å, c = 15.378(4) Å, β = 102.99(2)°, V = 3176.6 Å^3, Z = 4, D_x = 1.322 Mg·m^{-3}, λ(Cu Kα) = 1.541 84 Å, μ = 0.138 mm^{-1}, 293 K, R = 0.067 for 3017 reflections with $F > 3\sigma(F)$; Zn(5-NO_2-OEP)(CH_3OH) (**9**-CH_3OH), $C_{37}H_{47}N_5O_3Zn$, M_r = 675.2, monoclinic, $P2_1/c$, a = 10.540(8) Å, b = 14.240(12) Å, c = 23.625(16) Å, β = 101.39(5)°, V = 3476(4) Å^3, Z = 4, D_x = 1.290 Mg·m^{-3}, λ(Mo Kα) = 0.710 73 Å, μ = 0.749 mm^{-1}, 130 K, R = 0.106 for 3894 reflections with $F > 4\sigma(F)$.

Introduction

The aggregation properties of porphyrins are of central importance for the understanding of the chemistry of chlorophylls and metalloporphyrins *in vivo*, especially with respect to studies on antenna complexes and the "special pair" chlorophyll dimer in the bacterial photosynthetic reaction center.[2] This area has been extensively studied in solution, the most detailed experiments using NMR spectroscopy.[3,4]

More than 30 years ago, Woodward invoked[5] a qualitative model for the porphyrin macrocycle as a means of explaining its chemical reactivity at the 5-, 10-,15-, and 20- (*meso*-) positions, and in particular the enhanced reactivity of the 15- and 20-positions in chlorins toward electrophilic reagents. In this model (**1**), the four "pyrrole" subunits were visualized as being independent 6-π-electron systems, therefore necessitating a depletion of π-electron density at the 5-, 10-, 15- and 20-positions of the 22-π-system. For chlorins (dihydroporphyrins), the saturation of the ring-IV subunit resulted in an overall increase in the π-electron density at the 15- and 20-positions.

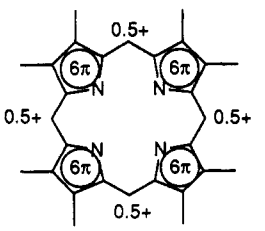

1

The porphyrin system is usually thought of as a completely delocalized π-system, but NMR studies of aggregation in porphyrins and chlorins have employed Woodward's hypothesis in order to explain the geometry of dimers and higher aggregates. These studies made use of the large magnetic anisotropy of the macrocyclic ring due to the interatomic ring current and thus required a precise ring-current model for a quantitative interpretation of the observed shifts. The double-dipole model developed by Abraham and Smith[6] has been applied successfully to the study of several substituted and unsubstituted porphyrins, their metal complexes,[7-12] and chlorophyll derivatives.[4,13] Ag-

(1) (a) University of California. (b) University of Notre Dame.
(2) Deisenhofer, J.; Michel, H. In *Chlorophylls*; Scheer, H., Ed.; CRC Press: Boca Raton, FL, 1991; p 613. Zuber, H.; Bruinsholz, R. A. In *Chlorophylls*; Scheer, H., Ed.; CRC Press: Boca Raton, FL, 1991; p 627. Bylina, E. J.; Youvan, D. C. In *Chlorophylls*; Scheer, H., Ed.; CRC Press: Boca Raton, FL, 1991; p 705.
(3) Katz, J. J. In *Porphyrins and Metalloporphyrins*; Smith, K. M., Ed.; Elsevier: Amsterdam, 1975; p 399. Katz, J. J.; Shipman, L. L.; Cotton, T. M.; Janson, T. R. In *The Porphyrins*; Dolphin, D., Ed.; Academic Press: New York, 1978; Vol. 5, p 402. Katz, J. J.; Bowman, M. K.; Michalski, T. J.; Worcester, D. L. In *Chlorophylls*; Scheer, H., Ed.; CRC Press: Boca Raton, FL, 1991; p 211. Scherz, A.; Rosenbach-Belkin, V.; Fisher, J. R. E. In *Chlorophylls*; Scheer, H., Ed.; CRC Press: Boca Raton, FL, 1991; p 237.
(4) Abraham, R. J.; Rowan, A. E. In *Chlorophylls*; Scheer, H., Ed.; CRC Press: Boca Raton, FL, 1991; p 797.
(5) Woodward, R. B.; Skaric, V. *J. Am. Chem. Soc.* **1961**, *83*, 4676.
(6) Abraham, R. J.; Fell, S. C. M.; Smith, K. M. *Org. Magn. Reson.* **1977**, *9*, 367. Abraham, R. J.; Bedford, G. R.; McNeillie, D.; Wright, B. *Org. Magn. Reson.* **1980**, *14*, 418. Abraham, R. J.; Smith, K. M.; Goff, D. A.; Lai, J.-J. *J. Am. Chem. Soc.* **1982**, *104*, 4332–4337. Smith, K. M.; Goff, D. A.; Abraham, R. J.; Plant, J. E. *Org. Magn. Reson.* **1983**, *21*, 505. Abraham, R. J.; Smith, K. M. *J. Am. Chem. Soc.* **1983**, *105*, 5734. Abraham, R. J.; Medforth, C. J.; Smith, K. M.; Goff, D. A.; Simpson, D. J. *J. Am. Chem. Soc.* **1987**, *109*, 4786. Abraham, R. J.; Medforth, C. J.; Mansfield, K. E.; Simpson, D. J.; Smith, K. M. *J. Chem. Soc., Perkin Trans. 2* **1988**, 1365.
(7) Abraham, R. J.; Eivazi, F.; Pearson, H.; Smith, K. M. *J. Chem. Soc., Chem. Commun.* **1976**, 698.
(8) Abraham, R. J.; Eivazi, F.; Pearson, H.; Smith, K. M. *J. Chem. Soc., Chem. Commun.* **1976**, 699.

0020-1669/93/1332-3134$04.00/0

gregation results in upfield shifts of specific resonances in the aggregated duplex, and the anisotropic effect can be quantified to yield accurate geometries in the dimers and higher oligomers. Aggregation effects have been observed in porphyrins, chlorins, and certain of their metal complexes, and the geometries of the aggregated species appear to be dependent upon $\pi-\pi$ donor–acceptor interactions between coplanar tetrapyrrole macrocycles.

Aggregation appears to be most prominently observable in porphyrins and metalloporphyrins bearing strongly electron-withdrawing groups at either the *meso*- or β-positions. It was proposed that the $\pi-\pi$ interactions are induced by polarization effects. For example, in porphyrins (**2**) substituted with an electronegative *meso*-substituent, electron deficiency is induced in the two pyrrole subunits flanking the *meso*-substituent, causing aggregation as shown (schematically) in **3** due to polarization. On the other hand, introduction of electronegative substituents at the pyrrole-subunit periphery (as in **4**) causes aggregates which have a generic structure as shown in **5**, or an alternative in which the upper ring is rotated 180° about the 5,15-axis.

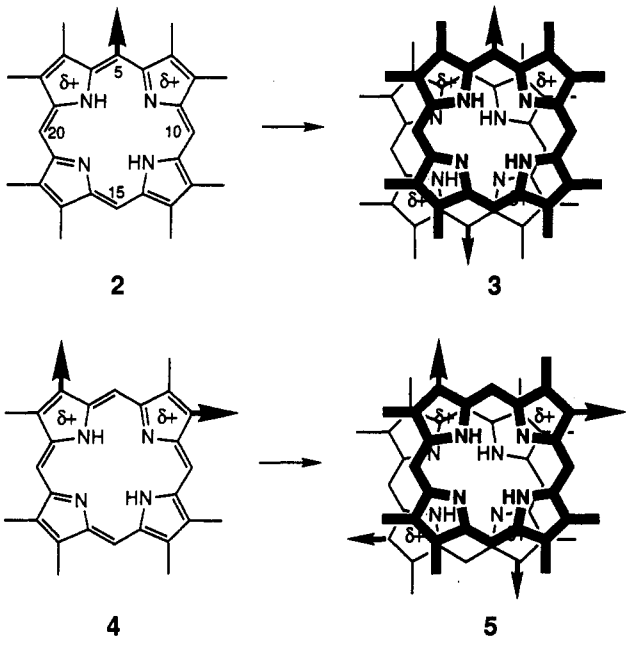

2 **3**

4 **5**

When metalloporphyrins are considered, the positively charged metal ion, particularly in full-shell metal ions such as Zn(II), where there is little $d\pi-p\pi$ back-bonding, tends to be attracted toward the electron-rich portion of the polarized system of its neighboring macrocycle, and this can have a dominant effect upon the geometry of the dimer or higher oligomers. Lack of $d\pi-p\pi$ back-bonding between the metal ion and its chelating porphyrin macrocycle can be measured in the low one-electron-electrochemical-oxidation potentials of the corresponding metalloporphyrin; thus, a correlation has been observed between electrochemical oxidation potentials and propensity for aggregation and, correspondingly, between the metal ion in the metalloporphyrin and degree of aggregation in a series of mesoporphyrin IX dimethyl ester derivatives.[8]

The dimeric structures formed are distinguished from those formed by magnesium porphyrins and chlorins, which aggregate mainly by coordination of oxo functions to the central metal.[3,7] The aggregated dimers are characterized by strong π-bonding or $\pi-\pi$-stacking interactions. If *meso*-substituents are present, which induce considerable charge polarization, the π-electron distribution around the ring will be very anisotropic and (i) the metal atom will complex to the most electron-rich part of the system and/or (ii) electron-rich areas will interact with electron-deficient areas. The influence of different substituents was shown by comparing the 5-acetoxy and 5-trifluoroacetoxy derivatives of octaethylporphyrin (OEP). While the zinc(II) complex of the former gave no indication for aggregation, the latter showed strong dimerization.[9] However, as shown with zinc(II) protoporphyrin IX and zinc(II) 3,8-dicyanodeuteroporphyrin IX dimethyl ester,[11] *meso*-substituents are not a necessary requirement for aggregation. Similar results have been obtained on the basis of ESR studies with iron(II),[14] iron (III),[15] and copper(II) porphyrins.[16] Recently the same rational was used to explain $\pi-\pi$-dimerization effects in dimeric porphyrins systems.[17]

In order to investigate the validity of this model in the solid state and to obtain more detailed structural information on such dimeric porphyrin structures, we have prepared a series of 5-nitro derivatives (**7**, **9**) of octaethylporphyrin (**6**) and studied their aggregation properties by X-ray crystallography.

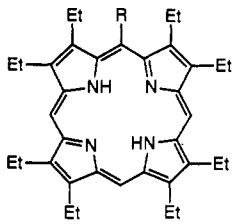

6 R = H
7 R = NO_2

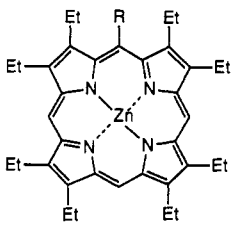

8 R = H
9 R = NO_2

Experimental Section

All compounds were synthesized and purified according to published procedures and gave satisfactory spectroscopic and elemental analysis data.[18]

Structure Determination of 2,3,7,8,12,13,17,18-Octaethyl-5-nitroporphyrin (7). Red parallelepipeds were grown by liquid diffusion of *n*-hexane into a concentrated solution of the porphyrin in methylene chloride. The crystals were immersed in hydrocarbon oil, and a single crystal was selected, mounted on a glass fiber, and placed in the low-temperature nitrogen stream.[19] A Siemens R3m/V automatic diffractometer with a graphite monochromator, equipped with a locally modified Siemens LT device and Mo Kα radiation (λ = 0.710 73 Å) was used for data collection. The compound crystallized in the triclinic space group $P\bar{1}$ with the cell parameters given in Table I. Cell constants were refined from 18 reflections with 19° ≤ 2θ ≤ 24°. Two standard reflections were measured every 198 reflections and showed only statistical variation (<1% intensity

(9) Abraham, R. J.; Barnett, G. H.; Hawkes, G. E.; Smith, K. M. *Tetrahedron* **1976**, *32*, 2949.
(10) Abraham, R. J.; Evans, B.; Smith, K. M. *Tetrahedron* **1978**, *34*, 1213.
(11) Smith, K. M. *Acc. Chem. Res.* **1979**, *12*, 374. Abraham, R. J.; Fell, S. C. M.; Pearson, H.; Smith, K. M. *Tetrahedron* **1979**, *35*, 1759.
(12) LaMar, G. N.; Viscio, D. B. *J. Am. Chem. Soc.* **1974**, *96*, 7354.
(13) Abraham, R. J.; Smith, K. M. *Tetrahedron Lett.* **1983**, *24*, 2681. Abraham, R. J.; Smith, K. M.; Goff, D. A.; Bobe, F. W. *J. Am. Chem. Soc.* **1985**, *107*, 1085. Abraham, R. J.; Goff, D. A.; Smith, K. M. *J. Chem. Soc., Perkin Trans. 1* **1988**, 2443.
(14) Kon, H.; Chikira, M.; Smith, K. M. *J. Chem. Soc., Dalton Trans.* **1981**, 1726.
(15) Chikira, M.; Kon, H.; Smith, K. M. *J. Chem. Soc., Chem. Commun.* **1978**, 906. Chikira, M.; Kon, H.; Smith, K. M. *J. Chem. Soc., Dalton Trans.* **1980**, 526.
(16) Boyd, P. D. W.; Smith, T. D.; Price, J. H.; Pilbrow, J. R. *J. Chem. Phys.* **1972**, *56*, 1253. Chikira, M.; Kon, H.; Hawley, R. A.; Smith, K. M. *J. Chem. Soc., Dalton Trans.* **1979**, 245.
(17) Hunter, C. A.; Sanders, J. K. M. *J. Am. Chem. Soc.* **1990**, *112*, 5525. Hunter, C. A.; Keighton, P.; Sanders, J. K. M. *J. Chem. Soc., Perkin Trans. 1* **1989**, 547. Senge, M. O.; Gerzevske, K. R.; Vicente, M. G. H.; Forsyth, T. P.; Smith, K. M. *Angew. Chem., Int. Ed. Engl.*, in press.
(18) Watanabe, E.; Nishimura, S.; Ogoshi, H. *Tetrahedron* **1975**, *31*, 1385. Evans, B.; Smith, K. M. *Tetrahedron Lett.* **1977**, *35*, 3079. Smith, K. M.; Barnett, G. H.; Evans, B.; Martynenko, Z. *J. Am. Chem. Soc.* **1979**, *101*, 5953.
(19) Hope, H. In *Experimental Organometallic Chemistry: A Practicum in Synthesis and Characterization*; Wayda, A. L., Darenbourg, M. Y., Eds.; ACS Symposium Series 357; American Chemical Society: Washington, DC, 1987; p 257.

Table I. Crystal Data and Data Collection Parameters for Compounds **7**, **9**-C_5H_5N, **9**, and **9**-CH_3OH

	7	**9**-C_5H_5N	**9**	**9**-CH_3OH
chem formula	$C_{36}H_{45}N_5O_2$	$C_{41}H_{48}N_6O_2Zn$	$C_{36}H_{43}N_5O_2Zn$	$C_{37}H_{47}N_5O_3Zn$
mol wt	579.8	722.6	643.15	675.2
space group	$P\bar{1}$	$P\bar{1}$	$P2_1/c$	$P2_1/c$
a, Å	9.374(3)	9.942(3)	9.721(3)	10.540(8)
b, Å	13.794(6)	10.722(4)	21.807(6)	14.240(12)
c, Å	14.221(4)	17.744(5)	15.378(4)	23.625(16)
α, deg	104.69(3)	81.74(3)	90	90
β, deg	106.39(2)	78.67(3)	102.99(2)	101.39(5)
γ, deg	104.57(3)	83.99(3)	90	90
V, Å^3	1599.7(10)	1829.5(8)	3176.6	3476(4)
Z	2	2	4	4
D_{calcd}, g·cm^{-3}	1.204	1.32	1.322	1.290
μ(Mo Kα), mm^{-1}	0.080	0.731	0.138 (Cu Kα)	0.749
λ, Å	0.710 73	0.710 73	1.541 84	0.710 73
T, K	130	293	293	130
R	0.078	0.063	0.067	0.106
R_w	0.123	0.061	0.088	0.137
S	1.05	1.58	2.50	1.30

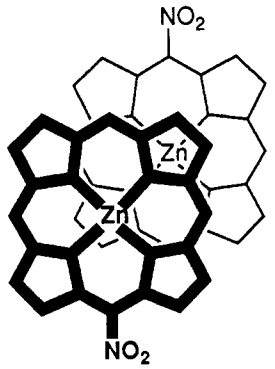

Figure 1. Schematic drawing of the dimer structure deduced by NMR experiments for (2,3,7,8,12,13,17,18-octaethyl-5-nitroporphyrinato)zinc(II) (**9**) in solution.

change). Data were corrected for Lorentz, polarization, and absorption effects;[20] extinction was disregarded.

The structure was solved via direct methods. The refinement was carried out by full-matrix least-squares procedures on $|F|$. The function minimized was $\sum w(F_o - F_c)^2$. The nitro group was found to be disordered over two opposite *meso*-positions and refinement with free split positions gave occupancies of 0.4:0.6 for the two nitro group positions. All non-hydrogen atoms were refined with anisotropic thermal parameters. Hydrogen atoms were included at calculated positions using a riding model (C–H distance 0.96 Å, N–H distance 0.9 Å, U_{iso}(H) = 0.04). No hydrogen atoms were added to the C10-position due to the disordering of the nitro group. The final cycle of refinement on $|F|$ included 418 independent parameters and converged with $R = 0.078$, $R_w = 0.123$, and $S = 1.05$. The data-to-parameter ratio was 8.0:1. The weighting scheme was defined as $w^{-1} = \sigma^2(F) + 0.0094F^2$; largest $\Delta/\sigma = 0.096$. The final difference Fourier synthesis gave $-0.43 \le \Delta\rho \le 0.26$ e·Å^{-3}. Further details of the data collection and refinement are given in the supplementary material.

Structure Determination of (Pyridine)(2,3,7,8,12,13,17,18-octaethyl-5-nitroporphyrinato)zinc(II) (9-C_5H_5N). Dark purple crystals were grown from pyridine. A suitable crystal was mounted on a Syntex P$\bar{1}$ diffractometer, and data were collected at 293 K using Mo Kα radiation (λ = 0.710 73 Å). The cell constants were obtained from a least-squares refinement of 28 reflections in the range $20° < 2\theta < 30°$ and are listed in Table I. The observed density, measured by flotation in a mixture of hexane/carbon tetrachloride, was found to be 1.31 g·cm^{-3}. Four standard reflections were measured every 2 h and showed a total decay of 6.3% in intensity over 286 h. No decay correction was applied. The data were corrected for Lorentz and polarization effects; absorption was disregarded.[21]

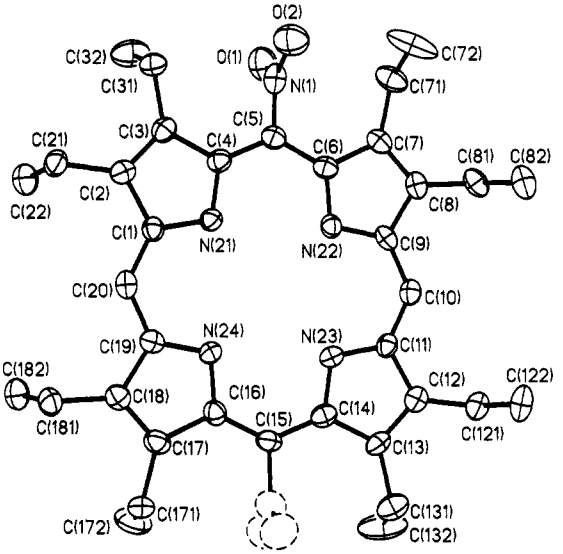

Figure 2. Molecular structure of 2,3,7,8,12,13,17,18-octaethyl-5-nitroporphyrin (**7**). Ellipsoids are drawn for 50% occupancy. The dashed atoms indicate the disordering of the nitro group.

The position of the zinc atom was determined by an unsharpened Patterson synthesis. All other atoms were located by direct methods followed by a series of difference Fourier calculations. The reflections were weighted using statistical weights plus a value for C_2, the factor used to downweight the intense reflections, equaling 0.04. All non-hydrogen atoms were refined with anisotropic thermal parameters. The hydrogen atom positions were calculated and given isotropic temperature factors 1 Å^2 greater than that of the heavy atom to which they are bonded. The refinement converged with $R = 0.063$, $R_w = 0.061$, and $S = 1.58$. After the final cycle, the largest peaks in the Fourier map were 0.9, 0.8, and 0.7 e·Å^{-3}. All were located near the Zn atom.

Structure Determination of (2,3,7,8,12,13,17,18-Octaethyl-5-nitroporphyrinato)zinc(II) (9). Crystals were grown from CH_2Cl_2/*n*-hexane. A deep purple, irregularly shaped crystal was mounted on a glass fiber in a random orientation. Preliminary examination and data collection were performed with Mo Kα radiation (λ = 0.710 73 Å) on a Syntex P$\bar{1}$

(20) Programs used in this study included the following. XABS, program for absorption correction, by H. Hope and B. Moezzi. The program obtains an absorption tensor from $F_o - F_c$ differences. See: Moezzi, B. Ph.D. Dissertation, University of California, Davis, 1987. Sheldrick, G. M. SHELXTL PLUS, Program for crystal structure solution. Universität Göttingen, Germany, 1989. Atomic scattering factors were used as supplied with SHELXTL. All calculations were performed on a Vaxstation 3200.

(21) Programs used in this study included local modifications of Main, Hull, Lessinger, Germain, Declerq, and Woolfson's MULTAN78, Jacobson's ALLS, Zalkin's FORDAP, Busing and Levy's ORFFE and ORLFS, and Johnson's ORTEP2. Atomic form factors were from: Cromer, D. T.; Mann, J. B. *Acta Crystallogr.* **1968**, *A24*, 321. Real and imaginary corrections for anomalous dispersions in the form factor of the zinc atom were from: Cromer, D. T.; Liberman, D. J. *J. Chem. Phys.* **1970**, *53*, 1891. Scattering factors for hydrogen were from: Stewart, R. F.; Davidson, E. R.; Simpson, W. T. *J. Chem. Phys.* **1965**, *42*, 3175. All calculations were performed on a VAX 11/730 or 3200 computer.

Table II. Atomic Coordinates ($\times 10^4$) and Equivalent Isotropic Displacement Coefficient ($Å^2 \times 10^3$) for 2,3,7,8,12,13,17,18-Octaethyl-5-nitroporphyrin (7)

atom	x	y	z	U(eq)[a]
N(21)	2365(3)	3823(2)	4682(2)	28(2)
N(22)	1652(4)	1635(3)	4447(2)	29(2)
N(23)	4175(3)	2169(2)	6551(2)	30(2)
N(24)	4855(3)	4367(2)	6798(2)	29(2)
C(1)	2956(5)	4909(3)	4982(3)	28(2)
C(2)	2097(5)	5222(3)	4171(3)	30(2)
C(21)	2355(5)	6355(3)	4225(3)	35(2)
C(22)	1563(6)	6892(4)	4894(4)	45(2)
C(3)	999(4)	4315(4)	3386(3)	31(2)
C(31)	-172(4)	4252(4)	2384(3)	36(2)
C(32)	-1633(5)	4467(5)	2512(4)	58(3)
C(4)	1183(4)	3434(3)	3720(3)	30(2)
C(5)	351(5)	2338(4)	3182(3)	30(2)
C(6)	571(4)	1491(4)	3505(3)	29(2)
C(7)	-313(4)	360(4)	2909(3)	31(2)
C(71)	-1530(5)	-119(4)	1818(3)	45(2)
C(72)	-809(7)	-283(6)	981(4)	83(4)
C(8)	257(5)	-174(3)	3521(3)	31(2)
C(81)	-231(5)	-1358(3)	3287(4)	38(2)
C(82)	830(6)	-1864(4)	2860(4)	47(3)
C(9)	1500(5)	635(3)	4478(3)	29(2)
C(10)	2391(5)	399(4)	5296(3)	30(2)
C(11)	3610(5)	1080(2)	6218(3)	28(2)
C(12)	4509(5)	764(3)	7002(3)	31(2)
C(121)	4306(5)	-367(3)	6932(4)	37(2)
C(122)	5242(6)	-824(4)	6333(4)	47(3)
C(13)	5615(5)	1672(4)	7800(3)	32(2)
C(131)	6763(5)	1667(5)	8775(3)	44(2)
C(132)	6090(7)	1674(7)	9632(4)	81(4)
C(14)	5374(3)	2565(3)	7507(2)	31(2)
C(15)	6165(5)	3665(4)	8049(3)	31(2)
C(16)	5928(4)	4522(4)	7747(2)	31(2)
C(17)	6790(4)	5662(4)	8346(3)	35(2)
C(171)	7953(5)	6182(4)	9454(3)	44(2)
C(172)	7155(7)	6296(6)	10251(4)	66(3)
C(18)	6238(5)	6176(3)	7711(3)	32(2)
C(181)	6730(5)	7358(3)	7930(4)	40(2)
C(182)	5681(6)	7881(4)	8350(4)	51(3)
C(19)	5040(4)	5365(2)	6753(3)	28(2)
C(20)	4181(5)	5600(4)	5919(3)	31(2)
N(1)	-828(9)	2061(6)	2224(7)	35(3)
O(1)	-2162(8)	2027(6)	2201(6)	55(3)
O(2)	-566(8)	1813(6)	1389(6)	56(3)
N(2')	7475(7)	3912(4)	9002(5)	52(3)
O(3')	7242(7)	3993(4)	9820(4)	75(3)
O(4')	8799(6)	4023(4)	8949(4)	72(3)

[a] Equivalent isotropic U defined as one-third of the trace of the orthogonalized U_{ij} tensor.

diffractometer. Indexing of 12 centered reflections from a rotation photograph yielded, after DeLaunay reduction, a monoclinic cell with $a = 4.86$ Å, $b = 21.89$ Å, $c = 15.09$ Å, and $\beta = 95.31°$. With the systematic absences $0k0$, $k = 2n$, and $h0l$, $h + l = 2n$, we deduced that the space group was $P2_1/n$ with $Z = 2$. Because of the weak scattering of the sample, it was moved to an Enraf-Nonius CAD4 computer-controlled κ-axis diffractometer equipped with a graphite crystal, incident-beam monochromator, and normal-focus Cu X-ray tube operating at 1200 W. Indexing of 14 automatically centered reflections from a rotation photograph yielded a cell with the 4.86-Å axis doubled. Careful reinspection of the axial photographs from the Syntex $P\bar{1}$ instrument confirmed faint evidence of the 9.7-Å axial length. Reindexing, centering, and least-squares refinement on the setting angles of 25 reflections with $20° < 2\theta < 31°$ led to the cell constants given in Table I. The observed density as determined by flotation in hexane/CCl_4 was 1.322 g·cm^{-3}. From the systematic absences $0k0$, $k = 2n$, and $h0l$, $l = 2n$, and from subsequent successful refinement, the space group was determined to be $P2_1/c$. Three standard reflections were measured every 2 h and showed large and irregular variations resulting in overall loss of intensity of 5.3%. The data were corrected for Lorentz and polarization effects, and absorption was corrected; extinction was disregarded.[21]

The structure was solved by direct methods, which gave the position of 25 macrocycle atoms. The remaining atoms were located in subsequent difference maps. The weighting scheme used was $w = 4F_o^2/\sigma^2(F_o^2) = 1/\sigma^2(F_o)$. The final cycle of refinement included 424 variable parameters and converged with $R = 0.067$, $R_w = 0.088$, and $S = 2.50$. The highest peak in the final difference map was 0.69 e·Å^{-3}. All other conditions are as described for the structure determination of **9**.

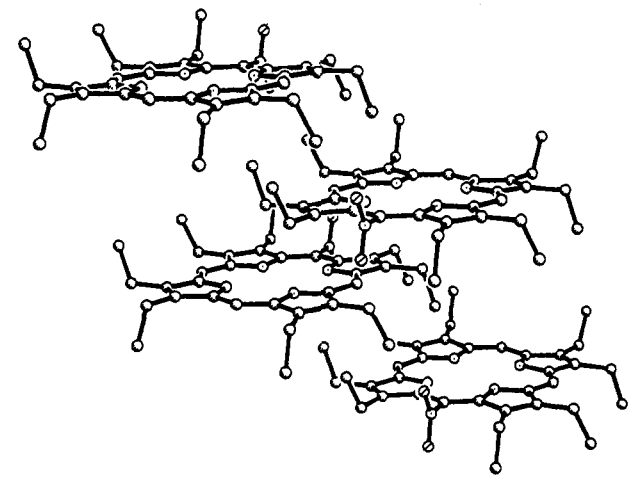

Figure 3. View of the molecular arrangement of **7** in the crystal. Only the nitro group position with the higher occupancy (0.6) is shown.

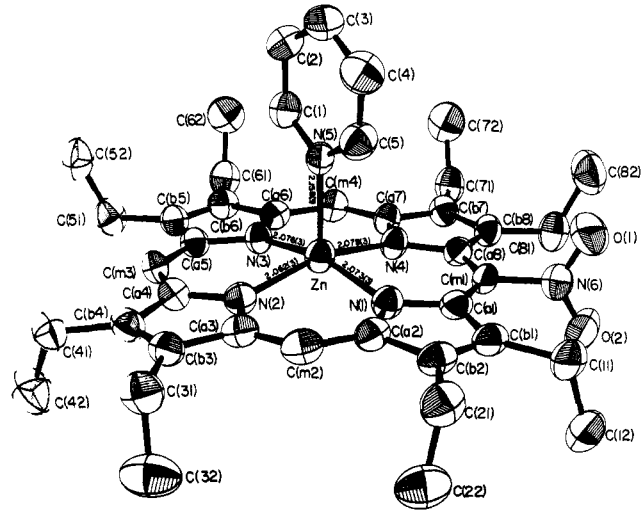

Figure 4. Molecular structure of (pyridine)(2,3,7,8,12,13,17,18-octaethyl-5-nitroporphyrinato)zinc(II) (9-C_5H_5N). Ellipsoids are drawn for 50% occupancy.

Structure Determination of (Methanol)(2,3,7,8,12,13,17,18-octaethyl-5-nitroporphyrinato)zinc(II) (9-CH_3OH). Brown cubes were grown by liquid diffusion of methanol into a concentrated solution of the porphyrin in chloroform. Cell constants were refined from 22 reflections with $18° \leq 2\theta \leq 23°$. Data were corrected for absorption; extinction was disregarded.[20]

The structure was solved via Patterson synthesis. The carbon atom of the methanol coordinated to the zinc atom was disordered and refined over three split positions with equal occupancy. Except for the axial methanol molecule, all non-hydrogen atoms were refined with anisotropic thermal parameters. The final cycle of refinement included 413 independent parameters and converged with $R = 0.106$, $R_w = 0.137$, and $S = 1.30$. H atoms were included at calculated positions using the riding model described for **2**. The axial methanol was refined without hydrogen atoms. The data-to-parameter ratio was 9.4:1. The weighting scheme was defined as $w^{-1} = \sigma^2(F) + 0.0087F^2$; largest $\Delta/\sigma = 0.048$. The final difference Fourier synthesis gave $-1.03 \leq \Delta\rho \leq$ e·Å^{-3}; the residual electron density was located near the Zn atom and the axial ligand. All other conditions are as described for the structure determination of **7**.

Results and Discussion

NMR evidence clearly showed that there are some prerequisites for aggregate formation. Asymmetric charge polarization in the ring system, induced by a central metal and enhanced by peripheral substituents or solely resulting from the presence of strongly

Table III. Fractional Coordinates[a] and Isotropic Equivalent Temperature Factors (Å²) for (Pyridine)(2,3,7,8,12,13,17,18-octaethyl-5-nitroporphyrinato)zinc(II) (9-C_5H_5N)

atom	x	y	z	B_{eq}[b]
Zn	0.83344(5)	0.45978(4)	0.23649(3)	3.55
O(1)	0.8142(4)	0.8268(3)	0.4252(2)	5.99
O(2)	0.7666(4)	0.9510(3)	0.3258(2)	5.91
N(1)	0.9600(3)	0.6026(3)	0.2342(2)	3.36
N(2)	0.9746(3)	0.3879(3)	0.1486(2)	3.33
N(3)	0.6900(3)	0.3521(3)	0.2114(2)	3.14
N(4)	0.6735(3)	0.5702(3)	0.2952(2)	3.25
N(5)	0.8933(3)	0.3385(3)	0.3344(2)	3.16
N(6)	0.7954(4)	0.8451(4)	0.3591(2)	4.38
C(a1)	0.9354(4)	0.7057(4)	0.2735(2)	3.31
C(a2)	1.0958(4)	0.6021(4)	0.1986(2)	3.61
C(a3)	1.1085(4)	0.4174(4)	0.1245(2)	3.66
C(a4)	0.9618(4)	0.2874(4)	0.1108(2)	3.51
C(a5)	0.7141(4)	0.2579(4)	0.1647(2)	3.33
C(a6)	0.5535(4)	0.3526(4)	0.2448(2)	3.34
C(a7)	0.5409(4)	0.5394(4)	0.3166(2)	3.35
C(a8)	0.6803(4)	0.6779(4)	0.3286(2)	3.31
C(b1)	1.0605(5)	0.7726(4)	0.2622(2)	3.59
C(b2)	1.1583(4)	0.7070(4)	0.2159(2)	3.56
C(b3)	1.1824(4)	0.3346(4)	0.0693(2)	3.59
C(b4)	1.0915(4)	0.2548(4)	0.0612(2)	3.70
C(b5)	0.5898(4)	0.1959(4)	0.1698(2)	3.45
C(b6)	0.4900(4)	0.2547(4)	0.2194(2)	3.60
C(b7)	0.4610(4)	0.6283(4)	0.3652(2)	3.70
C(b8)	0.5450(4)	0.7147(4)	0.3725(2)	3.58
C(m1)	0.8043(5)	0.7350(4)	0.3173(2)	3.27
C(m2)	1.1626(4)	0.5148(4)	0.1496(3)	3.73
C(m3)	0.8408(5)	0.2280(4)	0.1189(2)	3.50
C(m4)	0.4869(4)	0.4391(4)	0.2944(2)	3.48
C(1)	0.8377(5)	0.2305(4)	0.3618(3)	4.12
C(2)	0.8689(5)	0.1514(4)	0.4257(3)	4.52
C(3)	0.9641(5)	0.1853(5)	0.4629(3)	4.69
C(4)	1.0245(5)	0.2954(5)	0.4354(3)	5.20
C(5)	0.9869(5)	0.3695(4)	0.3714(3)	4.41
C(11)	1.0824(5)	0.8957(4)	0.2889(3)	4.29
C(12)	1.0583(6)	1.0104(4)	0.2310(3)	5.46
C(21)	1.3045(5)	0.7382(5)	0.1835(3)	4.82
C(22)	1.3267(5)	0.8013(5)	0.1004(3)	6.04
C(31)	1.3286(5)	0.3443(5)	0.0280(3)	4.64
C(32)	1.3425(6)	0.4433(6)	-0.0420(3)	6.84
C(41)	1.1142(5)	0.1526(4)	0.0087(3)	4.40
C(42)	1.0667(6)	0.1956(6)	-0.0667(3)	6.39
C(51)	0.5763(5)	0.0861(4)	0.1281(3)	4.30
C(52)	0.6071(6)	-0.0404(5)	0.1728(3)	5.72
C(61)	0.3434(5)	0.2223(4)	0.2477(3)	4.34
C(62)	0.3244(5)	0.1355(5)	0.3228(3)	5.76
C(71)	0.3106(5)	0.6195(4)	0.4020(3)	4.53
C(72)	0.2897(5)	0.5244(5)	0.4730(3)	6.12
C(81)	0.4974(5)	0.8269(4)	0.4172(3)	4.81
C(82)	0.5050(6)	0.8002(5)	0.5031(3)	6.51

[a] The estimated standard deviations of the least significant digits are given in parentheses. [b] Isotropic thermal parameter calculated from $B = 4[V^2 \det(\beta_{ij})]^{1/2}$.

electronegative substituents, was found to be a necessary requirement. When both metal and electronegative substituents are present, the aggregation in solution is particularly strong and easily observed by NMR.

One of the cases best studied by NMR involves mono-*meso*-substituted zinc(II) porphyrins. Such compounds have been used to study the influence of different side groups; e.g. a comparison of the 5-acetoxy and 5-trifluoroacetoxy derivatives of Zn^{II}(OEP) showed strong aggregation only in the latter case.[9] Due to highly resolved NMR signals, nitro derivatives of OEP have been used to delineate the dimer structure in solution in detail.[10] In principle two different orientations of the dimer are possible. One is the tail-to-tail dimer with the *meso*-substituents pointing in opposite directions; the other, the head-to-tail dimer with both *meso*-substituents on the same side. NMR evidence clearly showed that the nitroporphyrins (**9**) aggregate with their *meso*-substituents pointing in opposite directions as suggested by the tail-to-tail model. The geometry of the dimer as determined in solution is shown in Figure 1. The structure is characterized by an interplanar distance of 4.5 Å and a lateral shift (LS)[22] of the two zinc atoms of 1.5 Å. It should however be pointed out that NMR gives an averaged structure, since the situation in solution is fluid. The only case where a static situation was observed in solution is the bacteriochlorophyllide *d* dimer, which forms hydrogen bonds.[13]

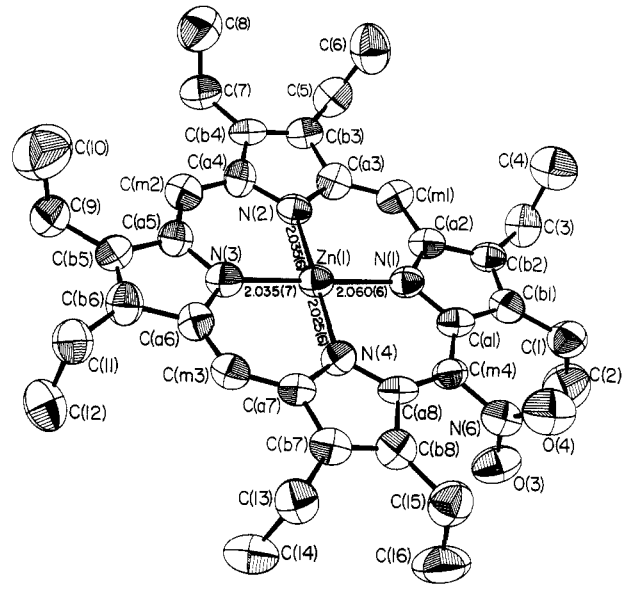

Figure 5. Molecular structure of (2,3,7,8,12,13,17,18-octaethyl-5-nitroporphyrinato)zinc(II) (**9**). Ellipsoids are drawn for 50% occupancy.

In the solid state such aggregates can easily be investigated by analysis of the molecular packing in the crystal. To investigate whether such π-bonded dimeric structures were also evident in the solid state, the structure of the metal-free 5-NO_2-OEP (**7**) was determined and is shown in Figure 2. Table I lists important structural data for all studied compounds, and Table VI compares selected bond lengths and angles. Isotropic thermal parameters and atomic coordinates for **7** are compiled in Table II. The molecule showed a disordering of the nitro group over the two opposite *meso*-positions. Analysis of the packing showed that no strong aggregation had taken place. Figure 3 gives a view of the molecular arrangement. Two different kinds of close packing are observed. Slight overlap of two pyrrole rings is observed in porphyrins in which the mean planes are 8.42 Å apart. This geometry is characterized by a center-to-center (Ct–Ct) distance of 9.374 Å, clearly showing no interaction. Nevertheless, a second type of stack with stronger overlap and closer spacing is observed. Two porphyrins have their mean planes spaced 3.46 Å apart with a Ct–Ct distance of 6.58 Å. This arrangement is characterized by a lateral shift (LS) of 6.58 Å. If only the nitro position with the higher occupancy is inspected, the nitro groups are oriented in opposite directions in neighboring molecules.

Scheidt and Lee have given a detailed analysis of the geometry of π–π interactions in porphyrin dimers.[23] It was found that a large number of porphyrins showed some kind of overlap of the aromatic system. General characteristics of π interactions in the solid state are mean plane separations of less than 4 Å and the formation of either aggregate type extended stacks or pairwise porphyrin interactions. On the basis of their lateral shift values, the types of aggregates can be grouped into three classes with weak, intermediate, or strong interactions. The last two had LS values varying around 3.5 and 1.5 Å, respectively. On this basis,

(22) The LS is calculated as [sin (slip angle) × Ct–Ct] as defined by Scheidt and Lee.[23] The slip angle is the angle between the mean plane of the rings and the Ct–Ct axis.

(23) Scheidt, W. R.; Lee, Y.-J. *Struct. Bonding* **1987**, *64*, 1.

Table IV. Fractional Coordinates[a] and Isotropic Equivalent Temperature Factors (Å^2) for (2,3,7,8,12,13,17,18-Octaethyl-5-nitroporphyrinato)zinc(II) (**9**)

atom	x	y	z	B_{eq}[b]
Zn	0.24325(11)	0.49955(7)	0.49706(8)	3.86
O(1)	0.128(4)	0.6680(17)	0.7126(26)	9.15
O(2)	-0.048(3)	0.6225(13)	0.7217(19)	6.26
O(3)	0.3743(8)	0.3201(4)	0.2856(6)	5.91
O(4)	0.5418(9)	0.3808(4)	0.2760(7)	7.22
N(1)	0.2298(6)	0.4948(3)	0.3616(4)	3.85
N(2)	0.0949(6)	0.56636(28)	0.4794(5)	3.82
N(3)	0.2595(6)	0.5051(3)	0.6311(4)	4.30
N(4)	0.3943(6)	0.43321(28)	0.5161(4)	3.81
N(5)	0.045(3)	0.6331(12)	0.7030(15)	2.19
N(6)	0.4395(9)	0.3698(5)	0.3029(7)	4.27
C(a1)	0.2997(8)	0.4562(4)	0.3156(6)	3.99
C(a2)	0.1432(8)	0.5295(4)	0.2990(6)	4.04
C(a3)	0.0279(8)	0.5929(4)	0.3981(6)	4.27
C(a4)	0.0407(8)	0.5978(4)	0.5420(6)	4.09
C(a5)	0.1832(9)	0.5434(4)	0.6757(5)	4.46
C(a6)	0.3480(8)	0.4710(4)	0.6955(5)	4.16
C(a7)	0.4644(7)	0.4102(3)	0.5962(5)	3.48
C(a8)	0.4451(8)	0.4032(3)	0.4519(6)	3.67
C(b1)	0.2539(8)	0.4672(4)	0.2202(6)	4.38
C(b2)	0.1592(8)	0.5136(3)	0.2108(5)	3.86
C(b3)	-0.0645(8)	0.6417(4)	0.4116(6)	4.08
C(b4)	-0.0590(8)	0.6437(3)	0.4993(6)	3.94
C(b5)	0.2311(9)	0.5334(4)	0.7710(6)	4.40
C(b6)	0.3297(9)	0.4897(5)	0.7837(5)	4.87
C(b7)	0.5601(8)	0.3646(4)	0.5834(6)	3.99
C(b8)	0.5521(8)	0.3572(4)	0.4938(6)	4.48
C(m1)	0.0495(7)	0.5759(4)	0.3134(6)	4.16
C(m2)	0.0820(8)	0.5858(4)	0.6350(6)	4.66
C(m3)	0.4457(8)	0.4292(4)	0.6780(6)	4.12
C(m4)	0.3966(8)	0.4124(3)	0.3602(5)	3.77
C(1)	0.2982(10)	0.4339(4)	0.1450(6)	5.60
C(2)	0.2075(14)	0.3799(6)	0.1087(8)	7.81
C(3)	0.0842(9)	0.5424(5)	0.1251(6)	5.44
C(4)	0.1560(10)	0.6021(5)	0.1049(7)	6.75
C(5)	-0.1490(9)	0.6798(5)	0.3401(6)	5.40
C(6)	-0.0640(11)	0.7288(6)	0.3090(7)	7.08
C(7)	-0.1366(8)	0.6857(4)	0.5473(6)	5.31
C(8)	-0.0614(12)	0.7486(5)	0.5673(7)	8.02
C(9)	0.1765(10)	0.5677(4)	0.8419(6)	5.41
C(10)	0.2547(14)	0.6273(6)	0.8663(9)	8.90
C(11)	0.4126(9)	0.4612(4)	0.8704(6)	5.46
C(12)	0.3564(10)	0.4026(5)	0.8950(6)	6.34
C(13)	0.6502(8)	0.3262(4)	0.6576(6)	4.97
C(14)	0.5669(10)	0.2746(4)	0.6911(7)	6.39
C(15)	0.6379(9)	0.3120(5)	0.4529(6)	5.63
C(16)	0.5689(12)	0.2503(4)	0.4398(7)	7.47

[a] The estimated standard deviations of the least significant digits are given in parentheses. [b] Isotropic thermal parameter calculated from $B = 4[V^2 \det(\beta_{ij})]^{1/2}$.

the aggregate observed in the free-base structure of **7** clearly belongs to the category with weak interactions. In solution no evidence for aggregation was found.[10] It should however be noted that the π effects in solution have to be very strong in order to be observed by NMR. Thus the fact that only weak interaction is observed in the crystal is in agreement with the spectroscopic results.

The structure of the zinc(II) complex of **9** when crystallized with pyridine is shown in Figure 4. Atomic coordinates and isotropic thermal coefficients are listed in Table III. The molecular structure shows clearly a typical five-coordinated zinc(II) porphyrin with a pyridine molecule as the fifth, axial ligand. The core of the macrocycle is characterized by Zn–N bond lengths of 2.073(3) Å, which is typical for five-coordinated Zn(II) porphyrins.[23] The axial ligand is bonded via the pyridine nitrogen with a bond length of 2.158(3) Å. This value is also typical for pyridine-ligated Zn(II) porphyrins, for which a range of 2.143(4)–2.200(3) Å has been described.[23] The closely related

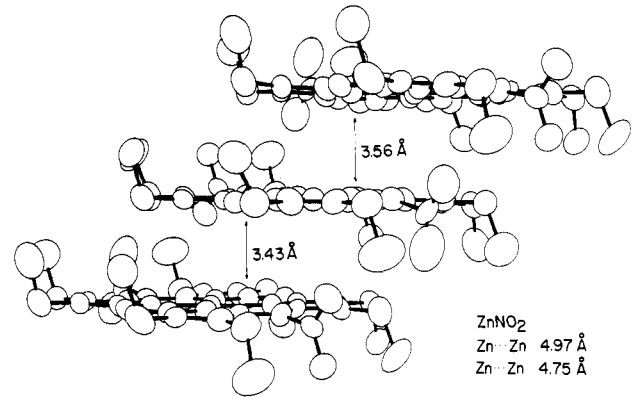

Figure 6. View of the molecular stacks of **9** in the crystal.

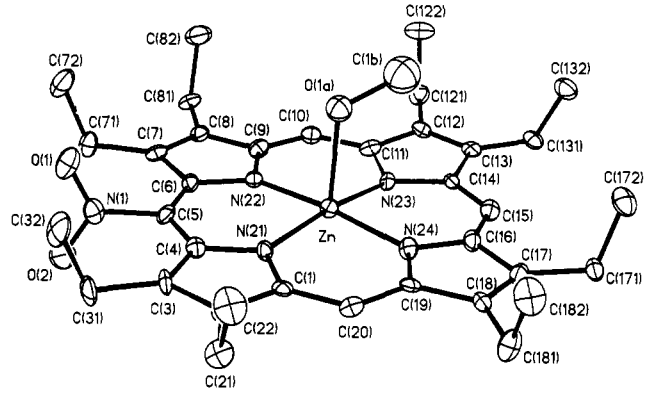

Figure 7. Molecular structure of (methanol)(2,3,7,8,12,13,17,18-octaethyl-5-nitroporphyrinato)zinc(II) (**9**-CH_3OH). Ellipsoids are drawn for 50% occupancy.

structure of Zn^{II}(OEP)(pyridine) shows M–N bond lengths of 2.067(6) Å and M–L_{ax} of 2.200(3) Å.[24]

Inspection of the molecular packing in the crystal reveals no unusual close contacts or any evidence for significant π–π interaction. The molecular structure thus shows a behavior like that observed for the porphyrin in solution, when treated with donor molecules (like pyrrolidine) to obtain monomers.

In order to obtain a more aggregated form, **9** was crystallized from CH_2Cl_2/*n*-hexane, degassed, and dried, to prevent deaggregation. Figure 5 shows the molecular structure of **9**, which crystallized with a planar four-coordinated zinc(II) without any axial ligand. Atomic coordinates and isotropic thermal parameters are listed in Table IV. As was the case in the structure of the free-base **7**, the present structure showed a disordering of the nitro group. The molecule very nearly possesses inversion symmetry. This symmetry is almost but not quite crystallographic, extending to the disordering of the nitro groups about the pseudo inversion center. Using manual adjustment of the occupancy factors for the two nitro groups, the occupancies refined to a ratio of 74:24.

Figure 6 shows a view of the molecular stacks formed by **9**. The closest intermolecular contact is 2.94 Å between O(2) and C(a1). There are two similar Zn–Zn intermolecular distances of 4.752(3) and 4.973(3) Å. The interplanar distances in the stacks are 3.43 and 3.56 Å. When the plane of the porphyrin core is viewed from above, the zinc atoms of adjacent molecules are laterally shifted by 3.29 Å (closer pair) or 3.47 Å (farther pair). The Zn–Zn–Zn angle is 177.87(6)°, and the molecules are tilted by about 44° toward the Zn–Zn vector. It is evident from the packing that the four-coordinated zinc(II) derivative forms a linear aggregate in the solid state. On the basis of the classification given earlier,[23] this type of interaction would be classified as being of intermediate

(24) Cullen, D. L.; Meyer, E. F., Jr. *Acta Crystallogr.* **1976**, *B32*, 2259.

Table V. Atomic Coordinates (×10⁴) and Equivalent Isotropic Displacement Coefficients (Å² × 10³) for (Methanol)(2,3,7,8,12,13,17,18-octaethyl-5-nitroporphyrinato)zinc(II) (**9**-CH_3OH)

atom	*x*	*y*	*z*	*U*(eq)[a]	atom	*x*	*y*	*z*	*U*(eq)[a]
Zn	1835(1)	139(1)	1(1)	25(1)	C(82)	1228(14)	−1339(9)	−2532(6)	58(5)
O(1A)	3811(8)	−478(6)	−33(3)	49(2)	C(9)	832(10)	−411(8)	−1256(4)	31(3)
C(1A)	3849(41)	−1302(29)	−392(17)	73(11)	C(10)	483(10)	−1308(7)	−1110(4)	29(3)
C(1B)	4115(50)	−1394(36)	227(20)	97(15)	C(11)	558(9)	−1696(7)	−560(4)	25(3)
C(1C)	4799(72)	−476(53)	551(29)	67(18)	C(12)	278(10)	−2646(7)	−416(4)	29(3)
N(21)	2403(8)	1526(5)	60(3)	24(3)	C(121)	−153(11)	−3394(8)	−848(4)	38(4)
N(22)	1338(8)	283(5)	−878(3)	23(3)	C(122)	951(12)	−3915(9)	−1032(6)	50(5)
N(23)	984(8)	−1167(5)	−55(3)	21(2)	C(13)	537(10)	−2727(7)	167(4)	28(3)
N(24)	2121(8)	54(5)	884(3)	28(3)	C(131)	464(10)	−3549(7)	523(4)	31(3)
C(1)	2871(9)	1994(6)	570(4)	23(3)	C(132)	1764(12)	−4027(7)	733(5)	44(4)
C(2)	3262(11)	2927(7)	458(4)	30(3)	C(14)	1005(10)	−1805(6)	396(4)	24(3)
C(21)	3889(11)	3613(8)	905(5)	40(4)	C(15)	1415(10)	−1570(7)	968(4)	32(4)
C(22)	5344(12)	3471(9)	1106(6)	55(5)	C(16)	1945(10)	−727(7)	1194(4)	30(3)
C(3)	3026(10)	3015(7)	−147(4)	28(3)	C(17)	2384(10)	−521(7)	1819(4)	29(3)
C(31)	3353(13)	3883(7)	−447(5)	42(4)	C(171)	2442(11)	−1244(7)	2282(4)	32(4)
C(32)	4732(14)	3868(9)	−571(6)	58(5)	C(172)	3553(12)	−1908(8)	2315(5)	45(4)
C(4)	2474(10)	2144(7)	−380(4)	27(3)	C(18)	2814(10)	367(6)	1861(4)	27(3)
C(5)	2040(10)	1863(7)	−964(4)	29(3)	C(181)	3377(11)	891(8)	2409(4)	41(4)
C(6)	1552(10)	1039(7)	−1213(4)	27(3)	C(182)	4813(12)	736(9)	2589(5)	54(5)
C(7)	1153(10)	815(7)	−1829(4)	28(3)	C(19)	2638(10)	720(7)	1274(4)	27(3)
C(71)	1209(11)	1398(8)	−2360(4)	38(4)	C(20)	2954(10)	1635(7)	1128(4)	28(3)
C(72)	2416(14)	1257(10)	−2599(5)	60(6)	N(1)	2296(10)	2587(6)	−1372(3)	37(3)
C(8)	700(10)	−83(7)	−1849(4)	27(3)	O(1)	3345(9)	2581(6)	−1528(3)	56(3)
C(81)	207(11)	−654(8)	−2380(4)	34(4)	O(2)	1437(9)	3164(6)	−1537(3)	56(3)

[a] Equivalent isotropic *U* defined as one-third of the trace of the orthogonalized U_{ij} tensor.

Table VI. Selected Bond Lengths (Å) and Bond Angles (deg) in **7**, **9**-C_5H_5N, **9**, and **9**-CH_3OH (Esd's in the Least Significant Digits in Parentheses)

atoms	**7**	**9**-C_5H_5N	**9**	**9**-CH_3OH	atoms	**7**	**9**-C_5H_5N	**9**	**9**-CH_3OH
Zn–L_{ax}		2.158(3)		2.276(9)	C(1)–C(2)–C(3)	107.9(4)	107.7(4)	107.1(7)	105.8(8)
Zn–N		2.073(3)	2.039(6)	2.055(8)	C(2)–C(3)–C(4)	106.2(3)	106.2(4)	106.1(8)	106.9(9)
N–C_a	1.364(4)	1.372(5)	1.377(10)	1.379(12)	N(21)–C(4)–C(3)	109.1(3)	109.7(3)	110.2(7)	109.9(8)
C(1)–C(2)	1.438(7)	1.446(5)	1.442(9)	1.430(12)	N(21)–C(4)–C(5)	122.5(4)	120.5(4)	121.3(8)	119.9(9)
C(1)–C(20)	1.394(5)	1.389(5)	1.412(10)	1.401(13)	C(3)–C(4)–C(5)	128.3(3)	129.8(4)	128.4(9)	130.2(9)
C(2)–C(3)	1.366(5)	1.346(6)	1.355(10)	1.406(13)	C(4)–C(5)–C(6)	127.7(4)	131.8(4)	128.7(8)	132.9(9)
C(3)–C(4)	1.444(7)	1.461(6)	1.454(11)	1.433(14)	N(22)–C(6)–C(5)	123.2(3)	120.8(4)	124.5(7)	120.8(8)
C(4)–C(5)	1.401(6)	1.400(6)	1.408(9)	1.422(13)	N(22)–C(6)–C(7)	111.1(4)	110.3(4)	110.0(8)	110.6(8)
C(5)–C(6)	1.399(8)	1.410(6)	1.398(11)	1.367(14)	C(5)–C(6)–C(7)	125.7(3)	128.9(4)	125.4(9)	128.5(9)
C(6)–C(7)	1.456(6)	1.466(5)	1.484(10)	1.468(13)	C(6)–C(7)–C(8)	106.0(3)	106.1(4)	103.4(8)	105.5(8)
C(7)–C(8)	1.358(7)	1.350(6)	1.373(12)	1.363(14)	C(7)–C(8)–C(9)	106.6(3)	107.2(4)	109.5(7)	107.5(8)
C(8)–C(9)	1.462(5)	1.438(5)	1.405(11)	1.457(14)	N(22)–C(9)–C(8)	110.5(4)	110.8(4)	110.3(8)	110.4(9)
C(9)–C(10)	1.391(7)	1.397(6)	1.376(11)	1.392(15)	N(22)–C(9)–C(10)	125.6(3)	124.6(4)	125.0(7)	126.1(9)
C(10)–C(11)	1.377(5)	1.387(6)	1.384(11)	1.399(14)	C(8)–C(9)–C(10)	123.9(4)	124.5(4)	109.5(7)	123.6(9)
C(11)–C(12)	1.430(6)	1.455(6)	1.466(10)	1.440(14)	C(9)–C(10)–C(11)	129.5(4)	128.7(4)	127.9(7)	128.6(9)
C(12)–C(13)	1.375(5)	1.349(6)	1.335(11)	1.355(14)	N(23)–C(11)–C(10)	126.5(4)	123.4(4)	124.1(8)	121.8(9)
C(13)–C(14)	1.446(8)	1.452(6)	1.452(11)	1.468(13)	N(23)–C(11)–C(12)	107.7(7)	110.8(4)	109.2(7)	110.4(8)
C(14)–C(15)	1.401(6)	1.393(6)	1.392(11)	1.377(13)	C(10)–C(11)–C(12)	125.8(3)	125.8(4)	126.5(8)	127.8(9)
C(15)–C(16)	1.403(8)	1.393(6)	1.420(12)	1.385(14)	C(11)–C(12)–C(13)	108.3(4)	106.3(4)	107.3(8)	108.1(8)
C(16)–C(17)	1.464(6)	1.445(5)	1.444(10)	1.485(13)	C(12)–C(13)–C(14)	106.3(3)	107.4(4)	108.1(8)	106.5(9)
C(17)–C(18)	1.354(7)	1.358(6)	1.337(12)	1.341(14)	N(23)–C(14)–C(13)	108.1(3)	110.0(4)	108.7(8)	110.3(8)
C(18)–C(19)	1.449(4)	1.445(5)	1.438(10)	1.453(13)	N(23)–C(14)–C(15)	122.3(4)	124.3(4)	125.2(8)	123.1(8)
C(19)–C(20)	1.395(7)	1.396(6)	1.415(11)	1.405(14)	C(13)–C(14)–C(15)	129.6(3)	125.6(4)	126.0(9)	126.6(9)
C–NO_2	1.441(7)	1.469(5)	1.406(13)	1.472(14)	C(14)–C(15)–C(16)	128.9(3)	127.3(4)	125.9(9)	127.9(10)
N–O	1.239(9)	1.222(5)	1.14(3)	1.230(14)	N(24)–C(16)–C(15)	121.9(3)	124.1(4)	123.0(8)	125.9(9)
L_{ax}–Zn–N		98.8(1)		93.9(3)	N(24)–C(16)–C(17)	111.3(4)	110.3(4)	110.4(8)	108.9(8)
N–Zn–N adj		88.7(1)	90.2(3)	89.7(3)	C(15)–C(16)–C(17)	126.7(3)	125.6(4)	126.5(9)	125.2(9)
N–Zn–N opp		162.4(1)	179.2(3)	172.2(3)	C(16)–C(17)–C(18)	105.4(3)	106.8(4)	107.9(9)	107.2(8)
Zn–N–C_a		126.9(3)		126.7(6)	C(17)–C(18)–C(19)	107.1(3)	106.6(4)	106.6(8)	106.1(8)
C(1)–N(21)–C(4)	108.3(4)	106.0(3)	106.0(6)	106.7(7)	N(24)–C(19)–C(18)	110.9(3)	110.4(4)	110.9(8)	111.4(8)
C(6)–N(22)–C(9)	105.8(3)	105.6(3)	106.7(6)	105.9(7)	N(24)–C(19)–C(20)	125.7(3)	123.6(4)	125.3(8)	124.3(9)
C(11)–N(23)–C(14)	109.6(3)	105.6(3)	106.6(6)	104.7(7)	C(18)–C(19)–C(20)	123.4(3)	125.9(4)	123.7(8)	124.3(8)
C(16)–N(24)–C(19)	105.3(3)	105.9(3)	104.1(7)	106.4(8)	C(1)–C(20)–C(19)	129.3(4)	123.9(4)	124.5(8)	126.6(9)
N(21)–C(1)–C(2)	108.4(3)	110.4(4)	110.6(7)	110.7(8)	C_a–C_m–NO_2	115.8(5)	114.1(4)	116(1)	113.4(8)
N(21)–C(1)–C(20)	125.8(4)	125.7(4)	127.4(8)	126.2(8)	C_m–N–O	119.2(6)	118.3(4)	114(3)	118.0(9)
C(2)–C(1)–C(20)	125.8(4)	123.9(4)	122.0(8)	123.2(8)	O–N–O	121.8(6)	123.4(4)	131(4)	123.9(9)

strength. Since solution studies clearly showed strong aggregation, a π–π-interaction structure of only "intermediate" strength might be considered a discrepancy from the solution results.

A very unusual structural feature was observed in the structure of **9** when crystallized from methylene chloride and methanol. The molecular structure of **9**-CH_3OH is shown in Figure 7; atomic coordinates and isotropic thermal parameters are listed in Table V. The molecule crystallized with a methanol molecule coordinated via its oxygen atom to the zinc atom. The Zn–N bond length is 2.055(8) Å, which is 0.02 Å shorter than the one observed in **9**-C_5H_5N. The Zn–O bond length is 2.276(9) Å, which agrees

(25) Glick, M. D.; Cohen, G. H.; Hoard, J. L. *J. Am. Chem. Soc.* **1967**, *89*, 1996. Golder, A. J.; Povey, D. C.; Silver, J.; Jassim, Q. A. A. *Acta Crystallogr.* **1990**, *C46*, 1210.
(26) Barkgia, K. M.; Berber, M. D.; Fajer, J.; Medforth, C. J.; Renner, M. W.; Smith, K. M. *J. Am. Chem. Soc.* **1990**, *112*, 8851.

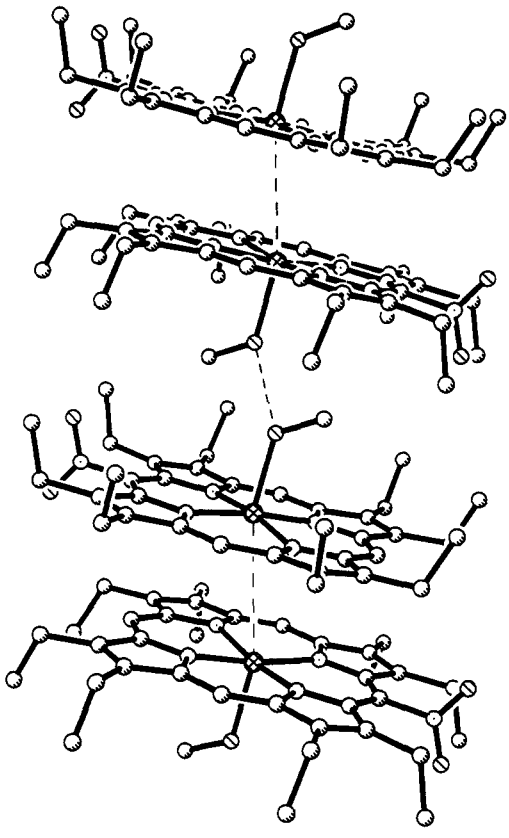

Figure 8. View of the aggregate structure observed for 9-CH_3OH.

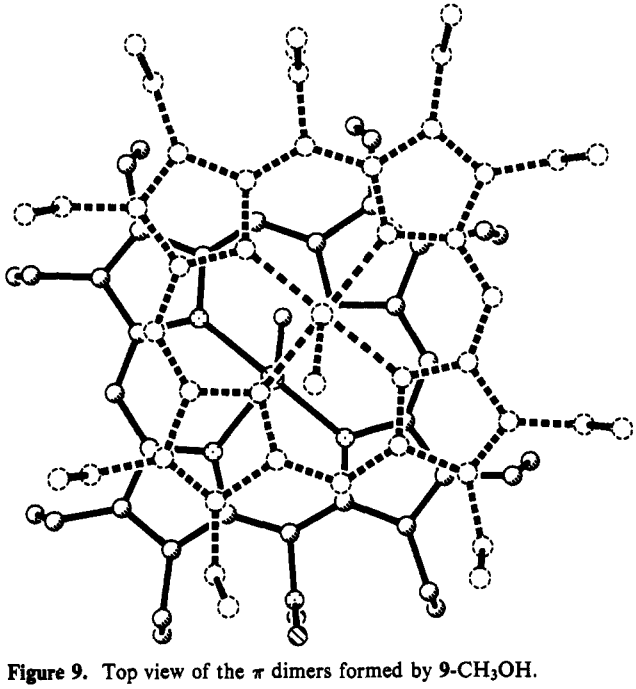

Figure 9. Top view of the π dimers formed by 9-CH_3OH.

well with the situation found in other Zn(II) porphyrins. ZnTPP·H_2O has a Zn–O bond length of 2.23(1) Å,[25] while the value found in (methanol)(2,3,7,8,12,13,17,18-octaethyl-5,10,15,20-tetraphenylporphyrinato)zinc(II) is 2.226(5) Å.[26]

Analysis of the molecular packing showed very unusual features (Figure 8). The recurring structural theme is a tetrameric group of molecules. Two molecules are held together via a hydrogen bond linking the oxygens of the two methanol molecules in neighboring units. Due to the disordering of the methanol CH_3 group, the hydrogen atom involved in this bond could not be located. However, the O–O distance of 2.83 Å clearly infers a hydrogen bond here. Due to the peculiar arrangement of the ethyl side chains, this dimeric structure has the ethyl groups of the two rings pointing toward each other, thus encasing the inner part with the axial methanols. Note that in this dimer the nitro groups point away from each other, too.

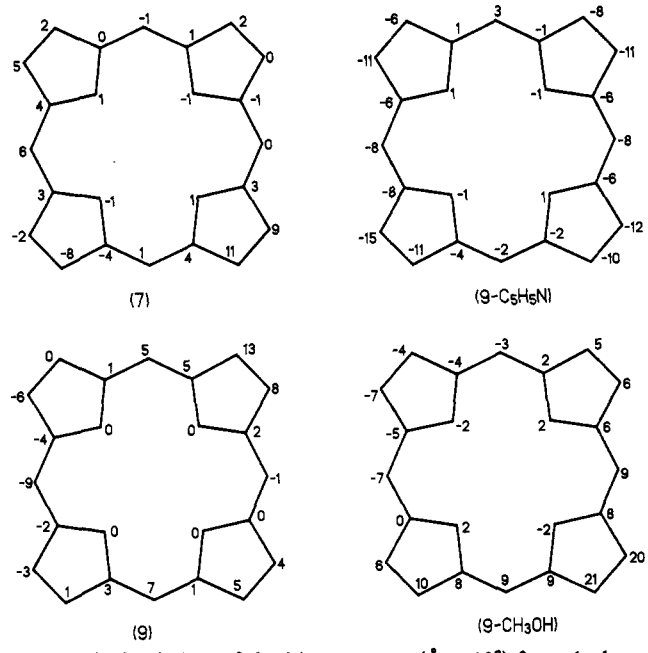

Figure 10. Deviations of the 24 core atoms (Å × 10^2) from the least-squares four-nitrogen plane in the structures of **7**, **9**-C_5H_5N, **9**, **9**-CH_3OH.

Besides the hydrogen-bonded dimer, a closely packed π–π dimer is also formed. This type of dimer is characterized by a strong overlap of the porphyrin ring systems (Figure 9). The two nitrogen planes are spaced 3.21 Å apart, and the Zn–Zn distance is 3.337 Å. Together with a slip angle of 39.4°, this leads to a lateral shift of the zinc atoms of 2.12 Å. This value is more than 1 Å smaller than that one observed in the structure of **9**. Thus the π interaction is much stronger in this case and brings this arrangement clearly into the group of strong interactions as defined earlier.[23] This structure might thus resemble more the situation in solution where, on the basis of NMR experiments, a lateral shift of about 1.5 Å was inferred.[9]

The same type of arrangement of the ethyl groups was found in the structure of the π–π dimer formed by $[Fe(OEP)NO)]^+$ [27] and $[Fe(OEP)(2\text{-}MeHIm)]^+$.[28] They exhibited lateral shifts of 1.5 and 1.43 Å, some of the smallest yet found, and a detailed analysis[29] of the Mössbauer spectra showed coupling of the two iron(III) ions through the π-system. The slightly larger lateral shift of 2.1 Å in **9**, compared to the ≈1.5 Å value usually observed for strongly interacting π–π-systems, is the probable result of the steric repulsion between the two *meso*-nitro groups.

The bond lengths and bond angles of most of the macrocycle atoms and peripheral substituents agree well with data observed for other related metalloporphyrins.[23] However, statistically significant differences are observed in the bond lengths of the core region of the porphyrins, which might reflect the aggregation effects.[30]

A question of some interest concerns the influence tightly packed porphyrin rings might have on each other conformationally. Figure 10 shows the deviations of the macrocycle atoms from the mean plane of the nitrogen atoms. No significant

(27) Scheidt, W. R.; Lee, Y. J.; Hatano, K. *J. Am. Chem. Soc.* **1984**, *106*, 3191.
(28) Scheidt, W. R.; Geiger, D. K.; Lee, Y. J.; Reed, C. A.; Lang G. *J. Am. Chem. Soc.* **1985**, *107*, 5693.
(29) Gupta, G. P.; Lang. G.; Scheidt, W. R.; Geiger, D. K., Reed, C. A. *J. Chem. Phys.* **1985**, *83*, 5945.
(30) Brennan, T. D.; Scheidt, W. R.; Shelnutt, J. A. *J. Am. Chem. Soc.* **1988**, *110*, 3919. Sparks, L. D.; Scheidt, W. R.; Shelnutt, J. A. *Inorg. Chem.* **1992**, *31*, 2191.

distortion is observed in the free base (**7**). The zinc(II) methanol complex **9**-CH_3OH shows however deviations of 0.2 Å for the pyrrole β-positions in one of the pyrrole rings, which might be an indication of conformational distortion in the aggregates. This kind of conformational interaction might of photobiological importance for e.g. photosynthetic chromophore aggregates.[31] No conformational distortion induced by steric interactions of the single nitro group with neighboring ethyl groups was found.

Our results clearly show that strong π–π dimeric or linear aggregates of nitro-substituted metalloporphyrins can be observed in the solid state. In agreement with the model developed for solutions on the basis of NMR results, the porphyrin molecule in question needs to have an asymmetric electron distribution in the system. The free-base porphyrin (**7**) showed only weak aggregation in the solid state, while two corresponding zinc(II) complexes showed intermediate (**9**) and strong dimerization (**9**-CH_3OH). A zinc(II) porphyrin with pyridine as an axial ligand (**9**-C_5H_5N)showed no aggregation and thus served as a model for the monomeric state in solution.

(31) Senge, M. O. *J. Photochem. Photobiol., B* **1992**, *16*, 3.

Acknowledgment. This work was supported by grants from the National Science Foundation (K.M.S., CHE-90-01381), the National Institutes of Health (W.R.S., NIH-GM-38401), and the Deutsche Forschungsgemeinschaft (M.O.S., Se543/1-1).

Supplementary Material Available: Listings of data collection parameters and complete bond lengths, bond angles, anisotropic thermal parameters, and hydrogen coordinates (18 pages). Ordering information is given on any current masthead page.